THE ASTROPHYSICAL JOURNAL, 371:L19–L22, 1991 April 10

ULTRAMASSIVE ($\sim 10^{11}\ M_\odot$) DARK CORE IN THE LUMINOUS INFRARED GALAXY NGC 6240?

JONATHAN BLAND-HAWTHORN
Department of Space Physics and Astronomy, Rice University, Houston, TX 77251-1892
ANDREW S. WILSON
Astronomy Program, University of Maryland, College Park, MD 20742
AND
R. BRENT TULLY
Institute for Astronomy, University of Hawaii, Honolulu, HI 96822
Received 1990 November 7; accepted 1991 January 22

ABSTRACT

We have obtained a detailed Hα velocity map of the superluminous ($\sim 6 \times 10^{11}\ L_\odot$), infrared galaxy NGC 6240 ($z = 0.0245$) with the Hawaii Imaging Fabry-Perot Interferometer (HIFI). The kinematic data reveal two dynamical systems (disks 1 and 2) that exhibit radically different rotation and are closely spaced in velocity (≈ 70 km s^{-1}) and position ($\approx 12''$, ≈ 5.7 kpc). Disk 1 (P.A. = 45° ± 5°) is roughly aligned with the major axis of the near-infrared continuum and exhibits flat rotation out to $\sim 20''$ in radius, centered on the double nucleus seen at optical, near-infrared, and radio wavelengths. The rotation turns over at $r_{t1} \approx 7''.2$ with a peak-to-peak velocity amplitude $\approx 280/\sin i_1$ km s^{-1}, where i_1 is the disk inclination. A preliminary analysis suggests $i_1 \simeq 70° \pm 7°$ although the effective beam of the filtered HIFI data (4″ FWHM) makes a reliable determination difficult.

The structure of disk 2 (P.A. = 155° ± 3°) is much more remarkable. The rotation curve comprises an unresolved, or marginally resolved, central velocity gradient with a peak-to-peak amplitude of $\approx 800/\sin i_2$ km s^{-1} within $r_{t2} < 2''.5$, and a faster than Keplerian drop-off outside r_{t2}. The peak rotation implies a compact mass M_2 greater than $4.5 \times 10^{10}\ M_\odot/\sin^2 i_2$ within a radius < 1.2 kpc. Presently, there are no observations of a luminous, compact counterpart to the core of disk 2 at radio, millimeter, infrared, or X-ray wavelengths, although our data show evidence for a weak optical continuum. We derive strict lower limits on the mass-to-light ratio from *UBVRIzK* photometry, in particular, $M_2/L_K > 3\ (M_\odot/L_\odot \sin^2 i_2)$ and $M_2/L_R > 60\ (M_\odot/L_\odot \sin^2 i_2)$. We believe that the observed gas motions provide strong evidence for the existence of an ultramassive, "dark matter" core or a compact dark object (e.g., dead or underfed quasar) in the NGC 6240 merger system.

Subject headings: galaxies: interactions — galaxies: internal motions — galaxies: nuclei — galaxies: structure — interferometry — spectrophotometry

1. INTRODUCTION

During the past decade, observational evidence from all wavebands has shown that the chaotic appearance of NGC 6240 is the result of a galactic collision (Fosbury & Wall 1979). When *IRAS* uncovered the existence of a class of galaxies that emit the bulk of their luminosity at far-infrared wavelengths (Soifer et al. 1984), it was soon realized that NGC 6240 is one such object (Wright, Joseph, & Meikle 1984). It is now known that all ultraluminous infrared systems ($\geq 10^{12}\ L_\odot$) have highly disturbed appearances (Sanders et al. 1988). In these galaxies, the molecular gas is centrally concentrated, constitutes a large fraction of the dynamical mass, and is thought to fuel the source of activity giving rise to the far-infrared luminosity.

In NGC 6240, the origin of the enormous infrared luminosity ($\sim 6 \times 10^{11} h_{75}^{-2}\ L_\odot$)[1] remains highly controversial. Opinions differ on the relative roles of large-scale shocks (Harwit et al. 1987), massive star formation (Condon et al. 1982; Soifer et al. 1984), or a "buried" active nucleus (Becklin & Wynn-Williams 1986) in heating the dust. The weakness of the Paα line in relation to the infrared luminosity (Depoy, Becklin, & Wynn-Williams 1986) suggests that the fraction of hot stars is considerably lower than in normal star formation regions within the Galaxy. The nature of the strong vibration-rotation H_2 lines from NGC 6240 (Lester, Harvey, & Carr 1988) has been widely discussed (e.g., Rieke et al. 1985; Harwit et al. 1987; Draine & Woods 1990). Recent λ2 μm imagery reveals that the H_2 is extended and distinct from the two continuum nuclei which would seem to favor large-scale shocks as the excitation mechanism (Fischer, Smith, & Glaccum 1990; Herbst et al. 1990). This inference is supported by recent simulations (Barnes & Hernquist 1991) which demonstrate that the observed nuclear gas concentration (Wang, Scoville, & Sanders 1991) can accumulate only after dissipating its orbital energy through strong radiative cooling in shocks. In this *Letter*, we report on the first complete kinematic maps for NGC 6240 from imaging Fabry-Perot observations, and we demonstrate that these data have important consequences for the origin and dynamics of this intriguing system.

2. OBSERVATIONS

The HIFI system (Bland & Tully 1989) was mounted at the Cassegrain focus of the University of Hawaii 2.2 m telescope on the nights of 1986 May 14–16. We observed 12 frames in photometric conditions for a total of 6 hr at 68 km s^{-1} (1.5 Å) increments across the Hα line, which is comparable to the

[1] A distance of 100 Mpc is adopted throughout this paper; h_{75} is Hubble's constant in units of 75 km s^{-1} Mpc^{-1}.

spectral resolution of the high-finesse (60) etalon, providing a velocity coverage of 820 km s^{-1}. The slight undersampling results in an effective velocity resolution of $\approx$100 km s^{-1}. A low read-out noise ($\sim 4e^-$), 385 × 576 format GEC CCD was placed at the image plane. The f/2 input beam yielded an image scale of 0.″85 pixel^{-1} and an overall field of view of 8′ × 5′. The HIFI data were calibrated and reduced following the guidelines of Bland & Tully (1989). These observations have been supplemented with Hα, [O III] λ4959, and Hβ narrow-band imagery using the Prime Focus CCD at the CTIO 4 m telescope on the nights of 1985 May 15–16 and 25–26. The RCA 512 × 320 CCD gave a plate scale of 0.″60 pixel^{-1} and a field of view of 5′ × 3′. The distribution of Hα line flux within the HIFI data compares well with the CCD imagery down to a limiting surface brightness of $\approx 10^{-17}$ ergs cm^{-2} s^{-1} arcsec^{-2}. However, in a few specific locations, especially near the bright, double nucleus, there is some confusion between line and continuum in that these are indistinguishable for lines broader than $\sim$500 km s^{-1} FWHM. Since our limited velocity range does not encompass the full velocity structure in NGC 6240, and in order to safeguard against possible interorder confusion, observations at three positions with a long-slit spectrograph were kindly obtained at our request by I. Pérez-Fournon on 1990 June 29–30 with the Calar Alto 3.5 m telescope. The Twin Spectrograph was used with the 108 Å mm^{-1} grating and a GEC CCD with 17 μm pixels providing 0.″63 pixel^{-1} and 1.8 Å pixel^{-1} along and perpendicular to the slit, respectively. The data have been corrected for cosmetic defects and for instrumental distortion; the sky and continuum were subtracted before fitting to the emission line profiles. W. C. Keel kindly provided additional *UBVRIzK* photometry that is discussed in detail elsewhere (Keel 1990).

3. RESULTS AND INTERPRETATION

The HIFI spectra show that while the Hα lines are both broad (>150 km s^{-1} FWHM) and display complex structure over the inner region, a bright core usually dominates the line profiles. These profiles have been fitted with Gaussian functions, and the resultant velocity field is presented in Figure 1. The gross distribution of the line flux above a surface brightness of $\approx 2 \times 10^{-17}$ ergs cm^{-2} s^{-1} arcsec^{-2} is characterized by two axes that run SW-NE and SE-NW. These axes cross north of the nucleus where the Hα lines are commonly found to have two components, although there is also evidence for multiple components in other regions. For these cases, the centroid velocity is given. Both photometric axes coincide with the steepest gradients through the velocity field, and the convex isovelocity contours, particularly in the SE and SW, are observed to align systematically along both gradients. The simplest interpretation is that these axes define the kinematic lines of nodes of two disks, each in differential rotation, that appear overlapping in projection. Figures 2*a* and 2*b* illustrate the observed radial velocities along P.A. 45° (disk 1) and along P.A. 155° (disk 2), respectively. Disk 1 shows an approximately flat rotation curve at large radii and is roughly centered on the bright, double nucleus observed at optical (Fried & Schulz 1983), infrared (Keel 1990), and radio wavelengths (Carral, Turner, & Ho 1990). The projected, total velocity amplitude is $\approx 280 \pm 10$ km s^{-1} at the turnover radius $r_{t1} \approx 7.''2$ and then remains roughly constant out to at least 20″. However, the form of the rotation curve to the NE is uncertain due to overlap with the NW side of disk 2. There is evidence for a mild warp ($\sim$15°) which may explain the antisymmetric kink

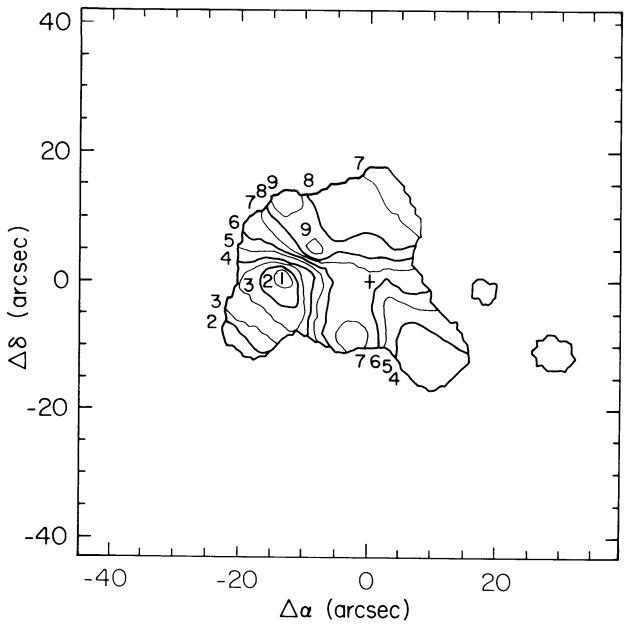

FIG. 1.—The Hα velocity field for an 85″ × 85″ field of view (north at top) sampled at 0.″85 increments. The outer boundary defines where the Hα surface brightness falls below 2 × 10^{-17} ergs cm^{-2} s^{-1} arcsec^{-2}. The origin, marked by a cross, coincides with the brighter peak of the compact, double nucleus. In order to increase the signal-to-noise ratio, the data have been convolved spatially with a 4″ FWHM Gaussian beam. The spectra were sampled at 68 km s^{-1} increments over a 820 km s^{-1} velocity range. The velocity contours in km s^{-1} are (1) 7120, (2) 7170, (3) 7220, (4) 7270, (5) 7320, (6) 7370 (systemic for disk 1), (7) 7420, (8) 7470, and (9) 7520.

in the rotation at a radius of 2″–4″. The kinematic major axis and uncertain disk inclination are P.A. $\simeq 45° \pm 5°$ and $i_1 \simeq 70° \pm 7°$, respectively.

The center of disk 2 (major axis P.A. $\simeq 155° \pm 3°$) is blueshifted by $\approx$70 km s^{-1} and offset by (11.″5E, 2.″5N) with respect to the double nucleus. The rotation curve for disk 2 from the HIFI data is significantly smeared by the low spatial resolution but exhibits a full amplitude of almost 600 km s^{-1} within a radius of 3″ and then drops rapidly. The long-slit measurements in Figure 2*b* show that, at higher spatial resolution ($\approx$1.″5 FWHM), the projected rotation is more extreme, with a full amplitude of $\approx$800 km s^{-1} at an observed turnover radius $r_{t2} \approx 2.''5$ ($\sim$1.2 kpc). Outside this radius, the decline in velocity is more rapid than Keplerian rotation on both sides of the center. The long-slit spectrogram presented in Figure 3 (Plate L3) shows that, as in disk 1, the [N II] λλ6548, 6584 and Hα line fluxes peak at the center of rotation (consistent with the Hα + [N II] image published by Heckman, Armus, & Miley 1987). Moreover, the [N II] λ6584/Hα ratio increases from typical values of 0.6–1.6 to values of $\approx$2 at the nucleus, which could arise from either metal enrichment during massive star evolution (Maeder 1983) or low-level, LINER-like activity (Heckman 1980). In Figure 2*b*, the two data sets show close agreement at the same resolution except in the NW where the long-slit measurements decrease faster with radius than the HIFI measurements. This reflects, in part, a small difference between the [N II] and Hα kinematics (Fig. 3) and inadequate velocity resolution to separate the two disks properly in the region of overlap.

In Figure 4 (Plate L4), the disk positions are overlaid onto the *K*-band isophotes and *B*+*V* image of NGC 6240. The orientation and radial extent of disk 1, particularly to the SW,

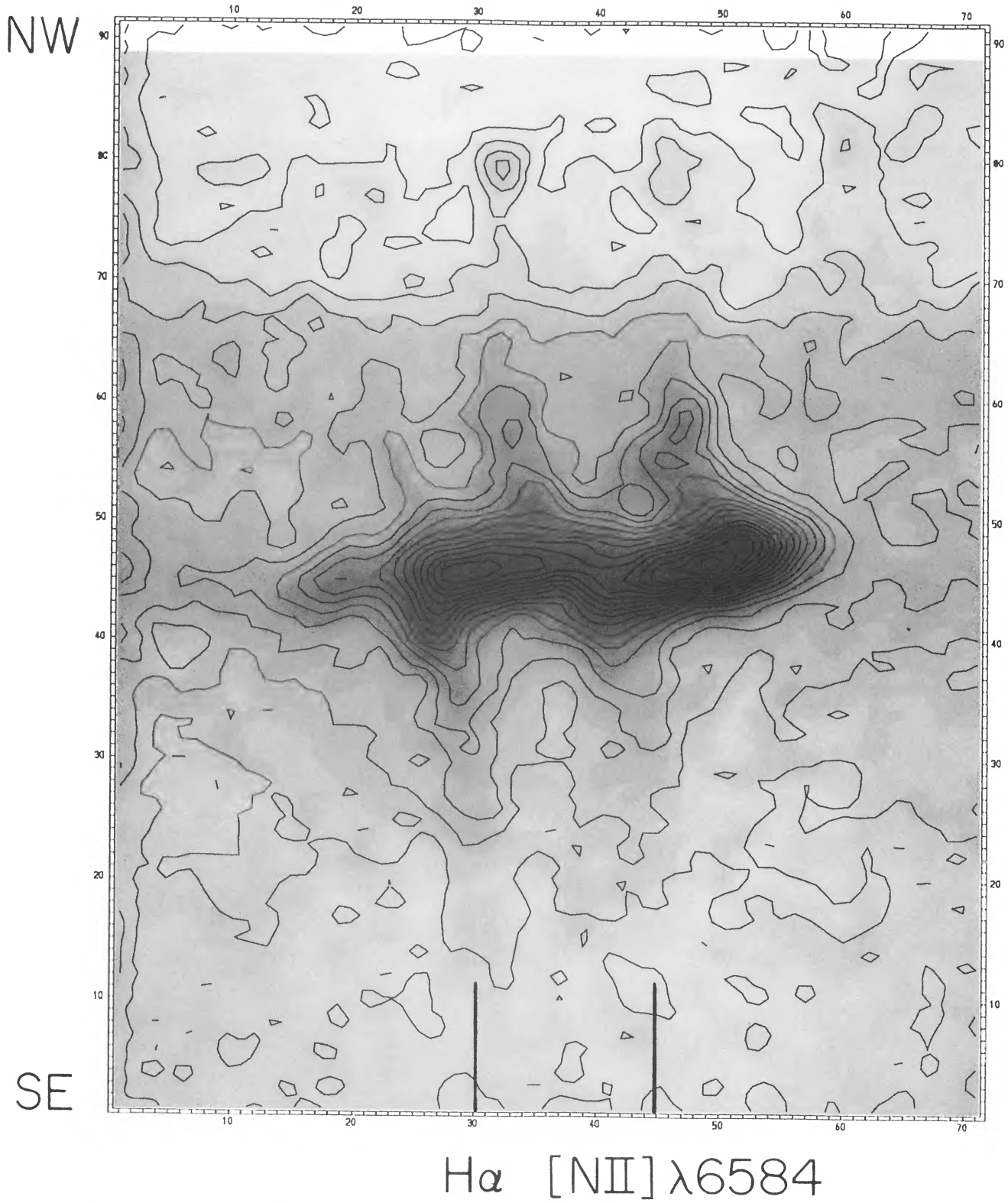

FIG. 3.—The long-slit spectrogram along the kinematic major axis of disk 2 (P.A. $\simeq 155°$) taken at the Calar Alto 3.5 m telescope. The horizontal axis covers 105 Å at 1.5 Å pixels^{-1} centered on Hα. The slit direction along the vertical axis is centered on the core of disk 2 and extends for 57″ from the SE (*bottom*) to the NW (*top*) at 0.″63 pixel^{-1}. The form of the rotation curve plotted in Fig. 2*b* is well defined. Notably, the core of disk 2 shows evidence for weak, diffuse continuum emission.

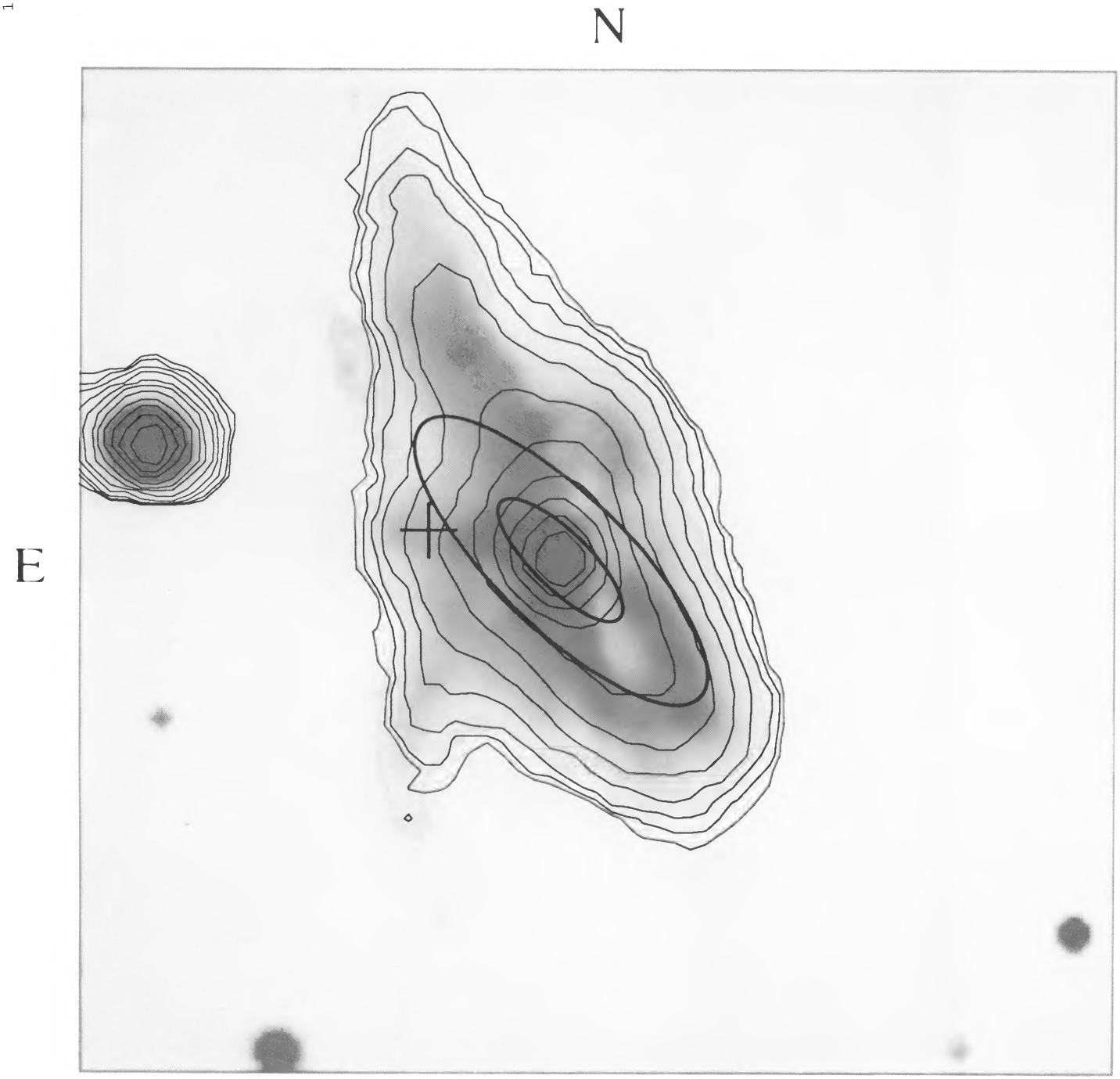

FIG. 4.—The positions of disks 1 and 2 and the orientation of disk 1 are shown on a photometric $B+V$ grayscale image of NGC 6240. The K continuum is overlaid using contours that have a resolution of 3".5 FWHM and are evenly spaced on a logarithmic scale between 5.6×10^{-14} and 1.8×10^{-11} ergs cm^{-2} s^{-1} arcsec^{-2}. The center of disk 2 is marked by a cross whose size is the diameter of the core. The outer ellipse for disk 1 shows the extent over which the rotation curve is observed (cf. Fig. 2*a*); the core size is shown by the inner ellipse. The core sizes in each disk are defined by the turnover radii r_{t1} and r_{t2}.

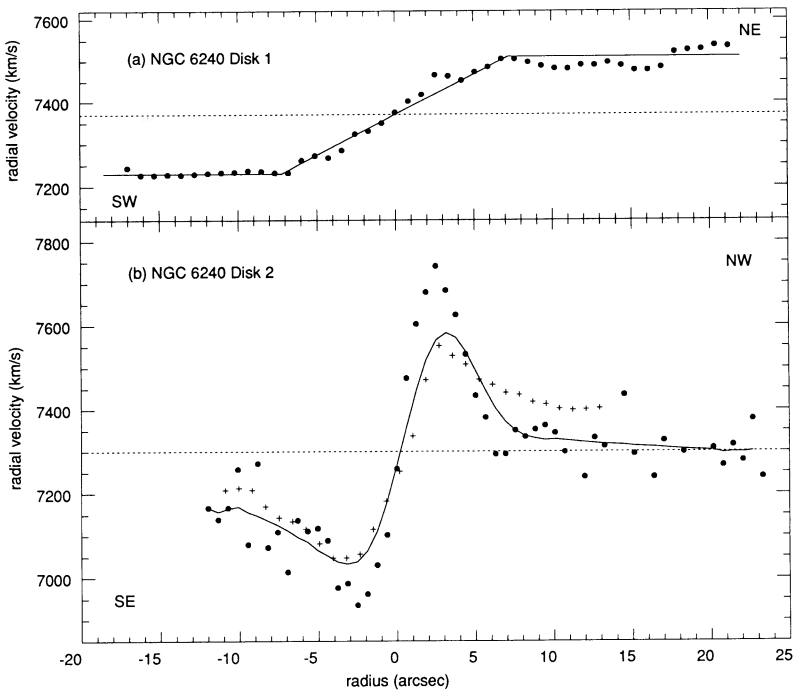

FIG. 2.—The steepest gradients through the HIFI Hα velocity field in Fig. 1 are found (*a*) along P.A. = 45° through the double nucleus (disk 1), and (*b*) along P.A. = 155° centered at an offset of (11″.5E, 2″.5N) from the double nucleus. Both rotation curves show inner regions that rise linearly with radius before turning over, beyond which the forms of the rotation are very different. The total, projected velocity amplitude in (*a*) is ≈ 280 km s^{-1} where the 1 σ error is ~ 20 km s^{-1} for the convolved data. In (*b*), the combined Hα + [N II] λ6584 measurements from the long-slit data are shown as filled circles: these have a total amplitude of ≈ 800 km s^{-1} at a turnover radius of 2″.5 (1.2 kpc). The Fabry-Perot measurements are marked as crosses and have an observed amplitude of ≈ 600 km s^{-1} significantly smaller than the long-slit values because of the lower spatial resolution of the former data. The continuous curve shows the effect of convolving the long-slit measurements with a 4″ FWHM beam and, except for a ~ 100 km s^{-1} deviation to the NW, displays a close resemblance to the HIFI measurements. In the absence of seeing ($\approx 1''.5$ FWHM), the central velocity gradient of disk 2 may be even steeper.

coincide well with the distribution of the *K* continuum brighter than 10^{-12} ergs cm^{-2} s^{-1} arcsec^{-2} although the photometric axis is closer to $\sim 40°$. Thus, disk 1 probably has a substantial stellar component that gives rise to the main body of 2 μm continuum. The intensity gradient changes to the NE where the long axis of the near-infrared continuum bends northward to P.A. $\sim 20°$ suggesting that the photometric axis of disk 1 is warped through a larger angle than implied by the kinematics. It has proved difficult to separate the two disks in the region of overlap as the local distribution in Hα surface brightness is highly complex. Consequently, we are unable to say whether the kinematics in the NE of disk 1 reflect the change in orientation in the *K* photometry here. In the *R*-band image (Keel 1990; Armus 1989), the core of disk 2 is located at the tip of the ridge that protrudes east of the double nucleus. In this region, the *K* isophotes exhibit a mild inflexion, suggesting a possible counterpart. By fitting a two-dimensional Gaussian profile to the bright star, we determine the FWHM of the point-spread function (PSF) for the *K*-band image to be $\approx 3''.5$. In order to obtain a strict upper limit on the *K* luminosity of the core, we scale and subtract the PSF convolved with a compact source (FWHM $\approx 2r_{t2}$) until a serious discontinuity occurs in the residual image. We deduce a *K* magnitude of ≥ 16.0 for the core as compared with ≈ 10.4 for the center of disk 1 (8″.5 diameter region) and ≈ 9.3 for the whole galaxy. (The latter values are in excellent agreement with Thronson et al. 1990.) We point out that as the central core of disk 2 may be unresolved in the long-slit data and since the inflexion in the *K*-band isophotes may be entirely unrelated to it, the intrinsic core luminosity in disk 2 is probably even lower than the strict upper limit of $L_K \sim 1.5 \times 10^{10}\ L_\odot$. Similar considerations apply to our derived upper limit for the core luminosity, $L_R \sim 7.5 \times 10^8\ L_\odot$, of disk 2 from the *R*-band photometry.

4. IMPLICATIONS

We are unable to find a luminous counterpart to the core of disk 2 in high-resolution maps from the radio (Carral et al. 1990), millimeter (Wang et al. 1991), near-infrared (Herbst et al. 1990), or X-ray (Rieke 1988) bands. Conceivably, the large *IRAS* beam (0′.76 × 4′.6) could hide a bright, compact source at the center of disk 2, although the listed *IRAS* position is very close to the center of disk 1, and the core of disk 2 lies close to the 95% confidence position ellipse (Fullmer & Lonsdale 1989). Wang et al. (1991) have observed NGC 6240 in the CO λ2.6 mm line and find $\sim 1 \times 10^{10}\ M_\odot$ of molecular gas concentrated within a diameter of roughly 8″ at the center of disk 1. The mass within this region from the rotation curve of disk 1 (Fig. 2*a*) is only $3 \times 10^9\ M_\odot/\sin^2 i_1$. However, if the broad (~ 700 km s^{-1} FWHM), nuclear lines reflect turbulent motion (Keel 1990), it is likely that the central gas in disk 1 is puffed up. After correcting for the pressure support, the total gravitating mass within the 2.6 mm beam is $\sim 4 \times 10^{10}\ M_\odot$; this confirms the conclusion of Wang et al. (1991) that the molecular gas is a substantial fraction of the dynamical mass. There is no evidence of CO emission at the core of disk 2. If the dust properties in NGC 6240 are similar to the Galaxy, then the visual extinction within a beam α in arcseconds is $A_V \sim (R/\alpha^2)(M_7/M_\odot)$ mag, where M_7 is the mass of gas in units of $10^7\ M_\odot$ and *R* is the selective extinction coefficient. Z. Wang (1990, private communication) estimates that no more than

$\approx 1 \times 10^9\ M_\odot$ (3 σ upper limit) could have escaped detection within the 7″ beam. If we conspire to place this mass of gas in front of the core of disk 2, the visual extinction could be as high as 12 mag, although this would imply a value of A_V an order of magnitude higher toward the center of disk 1. Our estimate of A_V suggests, however, that the core of disk 2 could be significantly obscured at near-infrared wavelengths, although this ignores the possibility of dust in clouds that do not radiate CO emission.

If the peak rotation is almost resolved at $r_{t2} \approx 2''.5$, the mass M_2 within this radius is $4.5 \times 10^{10}\ M_\odot/\sin^2 i_2$. If the isovelocity contours are matched to those of a planar disk in circular rotation, the derived inclination is $i_2 = 35° \pm 10°$. However, the confusion with disk 1 and the noncircular motions implied by the faster than Keplerian fall in rotation invalidate this method for determining the inclination. Our estimate of M_2 assumes that the rotation curve reflects dynamical equilibrium inside r_{t2} and that the tidal radius of disk 2 extends beyond r_{t2}. The quadrupole moment from M_1 may account for the fast drop-off in Figure 2*b*, although this depends on the relative positions and the spin orientations of the disks with respect to their orbital angular momentum. Our strict upper limits on the K and R luminosities indicate that $M_2/L_K > 3\,(M_\odot/L_\odot \sin^2 i_2)$ and $M_2/L_R > 60\,(M_\odot/L_\odot \sin^2 i_2)$. The core of disk 2 is somewhat darker than the M/L_V limit for the nucleus of M87 (Sargent et al. 1978), and much more massive. A supermassive black hole coalescing with disk 1 is one possible interpretation; higher resolution data are needed to see whether the rotational velocity in disk 2 continues to increase toward smaller radii than our resolution. Other possibilities include compact, dark stellar systems (e.g., highly evolved or brown dwarf stars). If we assume virial equilibrium, the stellar velocity dispersion $\langle V_* \rangle$ exceeds 800 km s^{-1} and gives a crossing time of $\tau_C \sim 3 \times 10^6$ yr. For a homogeneous cluster of N_* stars near the thermonuclear threshold ($\approx 0.08\ M_\odot$) with a dynamical cross section σ_*, the relaxation time ($\tau_R \sim \tau_C N_*/8 \ln N_*$) and the coalescence time ($\tau_s \sim 1/N_* \sigma_* \langle V_* \rangle$) are of order 10^{15-16} yr. If the core condensed through strong tidal interactions with disk 1, Barnes & Hernquist (1991) have shown that only dissipative matter settles easily to the center, after shedding angular momentum through large-scale shocks. This would tend to rule out collisionless systems, in particular, stars or putative "dark matter." However, if the true core radius of the cluster is < 100 pc and if the initial mass function is weighted strongly toward high-mass stars, the relaxation times may be short enough in the core for matter to coalesce and form a massive black hole (Murphy, Cohn, & Hut 1990). The flat rotation curve of disk 1 (see Fig. 2*a*) is usually attributed to a dark halo supporting the rotation (Caldwell & Ostriker 1981). On the assumption that $M_1 > M_2$, the two systems are expected to merge through dynamical friction on a time scale $\approx 2\pi(R_{\rm min}/V_{\rm orb})(M_1/M_2) \geq 2 \times 10^8$ yr where $R_{\rm min}$ is the separation of the disk centers and $V_{\rm orb}$ is the orbital velocity of M_2 (Binney & Tremaine 1987).

The central engines of quasars are commonly held to be supermassive ($\geq 10^8\ M_\odot$) black holes that radiate close to the Eddington limit. If one makes the usual association between radio-quiet quasars and powerful Seyferts (i.e., spirals), roughly one-third of all local L_* galaxies should possess a supermassive black hole (Begelman, Blandford, & Rees 1984). Thus, over half of all mergers now involve at least one spiral with a black hole. In one respect, it is not surprising that the kinematic detection of an *ultra*massive dark object ($\geq 10^{10}\ M_\odot$) has waited until now, since few mergers and none of the ultraluminous infrared systems ($\geq 10^{12}\ L_\odot$) have been mapped before. Moreover, contemporary imaging spectroscopic techniques at any wavelength are unlikely to detect the signature of a much less massive system in external galaxies because of the limited spatial resolution. Stockton (1990) has reviewed observations supporting the notion that at least some quasars may be triggered by strong dynamical interactions. The light profile of the ultraluminous infrared galaxy Arp 220 obeys an $r^{1/4}$ law at $\lambda 2$ μm (Wright et al. 1990) which presumably arises in the violent relaxation of the merging stellar systems (White 1979). If this is the ultimate fate of NGC 6240, then it may be that the dark core and the observed CO concentration will sink to the center, thus refueling the putative black hole and producing a short-lived quasar or a giant, radio elliptical galaxy. We expect high-resolution observations with the NASA Great Observatories to determine the specific nature of the core of disk 2.

J. B. H. and R. B. T. acknowledge partial funding through NSF grant AST 88-18900 that supports the HIFI "Nearby Active Galaxies" program. A. S. W. is supported by NSF grant AST 87-19207, NASA grant NAG 8-793, and a University of Maryland Graduate School Fellowship. We wish to acknowledge helpful comments from the referee and conversations with L. Armus, K. D. Borne, J. Goodman, L. Hernquist, J. Kormendy, F. C. Michel, B. W. Murphy, and J. C. Weisheit. We owe a considerable debt to W. C. Keel who graciously supplied much of the photometry and to I. Pérez-Fournon who obtained the long-slit observations.

REFERENCES

Armus, L. 1989, Ph.D. thesis, University of Maryland
Barnes, J. E., & Hernquist, L. 1991, ApJ, 370, L65
Becklin, E. E., & Wynn-Williams, C. G. 1986, in Star Formation in Galaxies (NASA CP-2466), p. 643
Begelman, M. C., Blandford, R. D., & Rees, M. J. 1984, Rev. Mod. Phys., 56, 255
Binney, J., & Tremaine, S. 1987, Galactic Dynamics (Princeton: Princeton University Press)
Bland, J., & Tully, R. B. 1989, AJ, 98, 723
Caldwell, N., & Ostriker, J. P. 1981, ApJ, 251, 61
Carral, P., Turner, J. L., & Ho, P. T. P. 1990, ApJ, 362, 434
Condon, J. J., Condon, M. A., Gisler, G., & Puschell, J. J. 1982, ApJ, 252, 102
Depoy, D. L., Becklin, E. E., & Wynn-Williams, C. G. 1986, ApJ, 307, 116
Draine, B. T., & Woods, D. T. 1990, ApJ, 363, 464
Fischer, J., Smith, H. A., & Glaccum, W. 1990, in Astrophysics with IR Arrays, ed. R. Elston (ASP Conf. Ser.), in press
Fosbury, R. A. E., & Wall, J. V. 1979, MNRAS, 189, 79
Fried, J. W., & Schulz, H. 1983, A&A, 118, 166
Fullmer, L., & Lonsdale, C. J. 1989, Cataloged Galaxies and Quasars Observed in the *IRAS* Survey (JPL D-1932)
Harwit, M., Houck, J. R., Soifer, B. T., & Palumbo, G. G. C. 1987, ApJ, 315, 28
Heckman, T. M. 1980, A&A, 87, 152
Heckman, T. M., Armus, L., & Miley, G. K. 1987, AJ, 93, 276
Herbst, T., Graham, J. R., Beckwith, S., Tsutsui, K., Soifer, B. T., & Mathews, K. 1990, AJ, in press
Keel, W. C. 1990, AJ, 100, 356
Lester, D. F., Harvey, P. M., & Carr, J. 1988, ApJ, 329, 641
Maeder, A. 1983, A&A, 120, 113
Murphy, B. W., Cohn, H. N., & Hut, P. 1990, MNRAS, 245, 335
Rieke, G. 1988, ApJ, 331, L5
Rieke, G. H., Cutri, R. M., Black, J. H., Kailey, W. F., McAlary, C. W., Lebofsky, M. J., & Elston, R. 1985, ApJ, 290, 116
Sanders, D. B., Soifer, B. T., Elias, J. H., Madore, B. F., Mathews, K., Neugebauer, G., & Scoville, N. Z. 1988, ApJ, 325, 74
Sargent, W. L. W., Young, P. J., Boksenberg, A., Shortridge, K., Lynds, C. R., & Hartwick, F. D. A. 1978, ApJ, 221, 731
Soifer, B. T., et al. 1984, ApJ, 278, L71
Stockton, A. 1990, in Dynamics and Interactions of Galaxies, ed. R. Wielen (Heidelberg: Springer), p. 440
Thronson, H., Majewski, S., Descartes, L., and Hereld, M. 1990, ApJ, 364, 456
Wang, Z., Scoville, N. Z., & Sanders, D. B. 1991, ApJ, 368, 112
White, S. D. M. 1979, MNRAS, 189, 831
Wright, G. S., James, P. A., Joseph, R. D., & McLean, I. S. 1990, Nature, 344, 417
Wright, G. S., Joseph, R. D., & Meikle, W. P. S. 1984, Nature, 309, 430